SUPPORTING INFORMATION

1 | NOTATION

In this manuscript, we consider 2D multi-channel images as vectors. Specifically, image $\boldsymbol{x} \in \mathbb{C}^{NC}$, with N pixels and C channels is formed by stacking the vectorized 2D channels in a column vector,

$$\boldsymbol{x} = \begin{bmatrix} \boldsymbol{x}_1 \\ \boldsymbol{x}_2 \\ \vdots \\ \boldsymbol{x}_C \end{bmatrix}. \tag{S1}$$

Operators which operate identically on the channels of an image or the pixels of an image can be represented as block matrices. For example, we can express applying the same matrix $\boldsymbol{A} \in \mathbb{C}^{N\times N}$ to every channel as,

$$(\boldsymbol{A} \otimes \boldsymbol{I}_C)\boldsymbol{x} = \begin{bmatrix} \boldsymbol{A} & & & \\ & \boldsymbol{A} & & \\ & & \ddots & \\ & & & \boldsymbol{A} \end{bmatrix} \begin{bmatrix} \boldsymbol{x}_1 \\ \boldsymbol{x}_2 \\ \vdots \\ \boldsymbol{x}_C \end{bmatrix} = \begin{bmatrix} \boldsymbol{A}\boldsymbol{x}_1 \\ \boldsymbol{A}\boldsymbol{x}_2 \\ \vdots \\ \boldsymbol{A}\boldsymbol{x}_C \end{bmatrix}, \tag{S2}$$

and we say that $(\boldsymbol{A} \otimes \boldsymbol{I}_C)$ is separable over channels or that $\underline{\boldsymbol{A}}$ is a channel-wise operator. Note that there is no natural ordering of arguments in the Kronecker product $(\cdot\otimes\cdot)$, and other papers may define their Kronecker product with arguments reverse compared to ours, without loss of generality.

Now suppose we have a matrix $(w_{ij}) = \boldsymbol{W} \in \mathbb{C}^{M\times C}$ which operates on image pixels $\boldsymbol{x}[i] \in \mathbb{C}^C,\ 1 \le i \le N$, i.e. $\boldsymbol{y}[i] = \boldsymbol{W}(\boldsymbol{x}[i]) \in \mathbb{C}^M$. We can conveniently express this as,

$$(\boldsymbol{I}_N \otimes \boldsymbol{W})\boldsymbol{x} = \begin{bmatrix} w_{11}I_N & w_{12}I_N & \cdots & w_{1C}I_N \\ w_{21}I_N & w_{22}I_N & \cdots & w_{2C}I_N \\ \vdots & \vdots & \ddots & \cdots \\ w_{M1}I_N & w_{M2}I_N & \cdots & w_{MC}I_N \end{bmatrix} \begin{bmatrix} \boldsymbol{x}_1 \\ \boldsymbol{x}_2 \\ \vdots \\ \boldsymbol{x}_C \end{bmatrix}. \tag{S3}$$

We say that $\overline{\boldsymbol{W}}$ is separable over pixels and is a pixel-wise operator. Note that $(\boldsymbol{I}_N \otimes \boldsymbol{W})$ also corresponds to a 1×1 kernel C to M channel convolution operator.

A nice aspect of this Kronecker product notation is the *mixed product property*, which states,

$$(\boldsymbol{A} \otimes \boldsymbol{B})(\boldsymbol{C} \otimes \boldsymbol{D}) = (\boldsymbol{A}\boldsymbol{C} \otimes \boldsymbol{B}\boldsymbol{D}) \tag{S4}$$

for matrices of compliant sizes. Hence, channel-wise and pixel-wise operators commute, i.e. $\overline{\boldsymbol{A}}\underline{\boldsymbol{B}} = \underline{\boldsymbol{B}}\overline{\boldsymbol{A}}$.

2 | SYNTHETIC NOISE GENERATION

We generated a single positive semi-definite noise-covariance matrix $\boldsymbol{\Sigma}$ for each volume using the following scheme,

$$\boldsymbol{L}_{ij} \sim \begin{cases} \mathcal{N}(\sigma_{\text{diag}},\, \sigma^2_{\text{jitter}}), & i = j \\ \mathcal{U}(-\sigma_{\text{corr}}/C,\, \sigma_{\text{corr}}/C), & \text{else} \end{cases} \tag{S5}$$

where $\boldsymbol{\Sigma} = \boldsymbol{L}\boldsymbol{L}^H$. Here, σ_{diag} determines the nominal noise-level of the image, σ_{jitter} introduces factors which contribute to a spatially varying noise in the coil-combined image, and σ_{corr} explicitly controls correlations between coil noise vectors, which also contribute to spatially noise variations in final image. We then generated our noisy volume with R repetitions via,

$$\boldsymbol{y}_{(r)} = \boldsymbol{S}\boldsymbol{x} + \overline{\boldsymbol{L}}\boldsymbol{b}_{(r)}, \quad \boldsymbol{b}_{(r)} \sim \mathcal{N}(0,\, \boldsymbol{I}),\ \forall\ r = 1, \ldots, R, \tag{S6}$$

with covariance matrix parameters $\sigma_{\text{diag}} = 0.15$, $\sigma_{\text{jitter}} = 0.02$, $\sigma_{\text{corr}} = 0.3$.

3 | NOISE WHITENING

It is standard to pre-whiten our data to improve optimize SNR upon coil-combination. To do so, $\boldsymbol{\Sigma}$ may be estimated directly from an acquisition without a patient in the scanner or indirectly through filtering methods (see main text Section 3.2). We form a whitening transform as a scaled Hermitian inverse square-root of the noise covariance matrix,

$$\boldsymbol{W} = \sigma\boldsymbol{\Sigma}^{-1/2}, \quad \sigma = \frac{\max|\boldsymbol{k}|}{\max|\overline{\boldsymbol{\Sigma}^{-1/2}}\boldsymbol{k}|} \tag{S7}$$

where σ is used to maintain the original signal value range. We obtain the whitened kspace via $\boldsymbol{k}' = \overline{\boldsymbol{W}}\boldsymbol{k}$, and whitened normalized coil-sensitivity map operator

$$\boldsymbol{R} = \underline{\boldsymbol{Z}}^{-1}\overline{\boldsymbol{W}}\boldsymbol{S} \tag{S8}$$

where $\boldsymbol{Z} = \sigma\sqrt{\boldsymbol{S}^H\overline{\boldsymbol{\Sigma}}^{-1}\boldsymbol{S}}$. Note that $\boldsymbol{Z}$ is diagonal and non-zero where $\boldsymbol{x}$ has data*. With this normalization, we perform coil-combination of the whitened image-domain data and compensate with the sensitivity profile,

$$\begin{aligned}
\boldsymbol{y} &= \boldsymbol{Z}^{-1}\boldsymbol{R}^H\underline{\boldsymbol{F}}^H\boldsymbol{k}' && \text{(S9)}\\
&= \boldsymbol{Z}^{-1}(\underline{\boldsymbol{Z}}^{-1}\overline{\boldsymbol{W}}\boldsymbol{S})^H\underline{\boldsymbol{F}}^H\overline{\boldsymbol{W}}\boldsymbol{k} && \text{(S10)}\\
&= \boldsymbol{Z}^{-1}\boldsymbol{S}^H\overline{\boldsymbol{W}}^H\underline{\boldsymbol{Z}}^{-1}\underline{\boldsymbol{F}}^H\overline{\boldsymbol{W}}\boldsymbol{k} && \text{(S11)}\\
&= \boldsymbol{Z}^{-2}\boldsymbol{S}^H(\boldsymbol{F}^H \otimes \boldsymbol{W}^H\boldsymbol{W})\boldsymbol{k} && \text{(S12)}\\
&= \boldsymbol{Z}^{-2}\boldsymbol{S}^H(\boldsymbol{F}^H \otimes \sigma^2\boldsymbol{\Sigma}^{-1})(\underline{\boldsymbol{F}}\boldsymbol{S}\boldsymbol{x} + \boldsymbol{\xi}) && \text{(S13)}\\
&= \sigma^2\boldsymbol{Z}^{-2}\boldsymbol{S}^H\overline{\boldsymbol{\Sigma}}^{-1}(\boldsymbol{S}\boldsymbol{x} + \boldsymbol{\xi}) && \text{(S14)}\\
&= (\boldsymbol{S}^H\overline{\boldsymbol{\Sigma}}^{-1}\boldsymbol{S})^{-1}(\boldsymbol{S}^H\overline{\boldsymbol{\Sigma}}^{-1}\boldsymbol{S}\boldsymbol{x} + \boldsymbol{S}^H\overline{\boldsymbol{\Sigma}}^{-1}\boldsymbol{\xi}) && \text{(S15)}\\
&= \boldsymbol{x} + (\boldsymbol{S}^H\overline{\boldsymbol{\Sigma}}^{-1}\boldsymbol{S})^{-1}\boldsymbol{S}^H\overline{\boldsymbol{\Sigma}}^{-1}\boldsymbol{\xi} && \text{(S16)}\\
&= \boldsymbol{x} + \boldsymbol{\xi}'_w, && \text{(S17)}
\end{aligned}$$

*This allows us to perform division sensibly by defining $0/0 \equiv 0$

where $\text{Cov}(\boldsymbol{\xi}'_w) = (\boldsymbol{S}^H\overline{\boldsymbol{\Sigma}}^{-1}\boldsymbol{S})^{-1} = \sigma^2\boldsymbol{Z}^{-2}$. Keeping track of the sensitivity compensation $\boldsymbol{Z}$ enables us to evaluate quantitative metrics (e.g. NRMSE, SSIM) with respect to our ground-truth data.

4 | NOISE-LEVEL FORMULA DERIVATIONS

4.1 | Verification of Correctness

Throughout this manuscript, we refer to the "noise-level" of coil-combined MRI signals. In general, an image contaminated with Gaussian-noise may have an arbitrary noise-covariance matrix associated with it, where non-zeros off the matrix's diagonal would express correlations between noise in different spatial locations in the image. We may still refer to noise-level as the square-root of the diagonal of the covariance matrix, which expresses the noise-power in each spatial location regardless of spatial correlations.

In this section we provide derivations for the noise-level of coil-combined image-domain MRI. The correctness of these formulas was verified empirically via simulation. In simulation, an empirical noise-level map may be obtained as follows. Consider an image $\boldsymbol{\mu}$ which we contaminate with zero-mean Gaussian resulting in noisy-image $\boldsymbol{y} \sim \mathcal{N}(\boldsymbol{\mu}, \boldsymbol{\Sigma})$. This image $\boldsymbol{y}$ may be obtained in some complicated way, such as contaminating $\boldsymbol{\mu}$ with noise in k-space followed by inverse Fourier-transform and coil-combination, and even involving some k-space interpolation. If we generate R such realizations of these images with noise following the same distribution, $\{\boldsymbol{y}_{(r)}\}_{r=1}^{R}$, we may then obtain an empirical noise-level map via computing a sample standard-deviation pixel-wise over the repetition dimension,

$$\boldsymbol{\sigma}_{\text{emp}} = \sqrt{\frac{\sum_{r=1}^{R}|\boldsymbol{y}_{(r)} - \boldsymbol{\mu}|^2}{R-1}}. \tag{S18}$$

As R increases, this empirical noise-level will tend to the true noise-level.

In the following sections, we present derviations for our noise-level formulas presented in the theory section of the manuscript.

4.2 | Fully-Sampled Data

For the fully sampled case, we have

$$\boldsymbol{y} = \boldsymbol{S}^H\underline{\boldsymbol{F}}^H\boldsymbol{k}, \tag{S19}$$

where $\boldsymbol{k} \sim \mathcal{N}(\boldsymbol{\mu}, \overline{\boldsymbol{\Sigma}})$. Hence, we have,

$$\boldsymbol{y} \sim \mathcal{N}(\boldsymbol{S}^H\underline{\boldsymbol{F}}^H\boldsymbol{\mu},\, \boldsymbol{S}^H\underline{\boldsymbol{F}}^H\overline{\boldsymbol{\Sigma}}\underline{\boldsymbol{F}}\boldsymbol{S}) = \mathcal{N}(\boldsymbol{x},\, \boldsymbol{S}^H\overline{\boldsymbol{\Sigma}}\boldsymbol{S}), \tag{S20}$$

where the simplification is a direct result of the mixed-product property of the Kronecker product and the normalization of sensitivity map operator $\boldsymbol{S}$.

Claim: $\boldsymbol{S}^H\overline{\boldsymbol{\Sigma}}\boldsymbol{S}$ is a diagonal matrix. We can show this by seeing that integer translates of the impulse signal, $\boldsymbol{e}_i$, form the eigen basis of this matrix, for all i:

$$\begin{aligned}(\boldsymbol{S}^H\overline{\boldsymbol{\Sigma}}\boldsymbol{S})\boldsymbol{e}_i &= (\boldsymbol{S}^H\overline{\boldsymbol{\Sigma}})(\boldsymbol{S}\boldsymbol{e}_i)\\ &= \boldsymbol{S}^H\overline{\boldsymbol{\Sigma}}(\boldsymbol{s}[i] \circ \boldsymbol{e}_i)\\ &= \boldsymbol{S}^H((\boldsymbol{\Sigma}\boldsymbol{s}[i]) \circ \boldsymbol{e}_i)\\ &= (\boldsymbol{s}[i]^H\boldsymbol{\Sigma}\boldsymbol{s}[i])\boldsymbol{e}_i,\end{aligned}$$

hence the noise covariance matrix is diagonal and given by $\boldsymbol{S}^H\overline{\boldsymbol{\Sigma}}\boldsymbol{S} = \mathbf{diag}(\boldsymbol{S}^H\overline{\boldsymbol{\Sigma}}\boldsymbol{s})$.

4.3 | GRAPPA-Reconstructed Data

In the case of subsampled k-space data reconstructed with linear-operator $\boldsymbol{G}^H$ (e.g. GRAPPA), we have

$$\boldsymbol{y} = \boldsymbol{S}^H\underline{\boldsymbol{F}}^H\boldsymbol{G}^H\underline{\boldsymbol{I}}_{\Omega}^T\boldsymbol{k}, \tag{S21}$$

where $\boldsymbol{k} \sim \mathcal{N}(\boldsymbol{\mu}, \overline{\boldsymbol{\Sigma}})$ and $\boldsymbol{\mu} \in \mathbb{C}^{N_s C}$ is the subsampled ground-truth k-space signal ($N_s < N$). Hence we have,

$$\boldsymbol{y} \sim \mathcal{N}(\boldsymbol{S}^H\underline{\boldsymbol{F}}^H\boldsymbol{G}^H\underline{\boldsymbol{I}}_{\Omega}^T\boldsymbol{\mu},\, \boldsymbol{S}^H\underline{\boldsymbol{F}}^H\boldsymbol{G}^H(\boldsymbol{M}_{\Omega} \otimes \boldsymbol{\Sigma})\boldsymbol{G}\underline{\boldsymbol{F}}\boldsymbol{S}). \tag{S22}$$

It is not immediately clear from (S22) what the noise-level of this reconstruction is, or what the structure of the noise-covariance matrix is in general.

In the case of GRAPPA with uniform acceleration rate A (without ACS inclusion), the interpolation operator may be written as a convolution, i.e. $\boldsymbol{G}^H = \boldsymbol{G}^H_{\text{conv}}$. Note that although GRAPPA typically employs linear convolution, for the purposes of analysis we may treat it as employing circular convolution due to the small kernel-sizes used in GRAPPA (ex. 3×3) and the low signal energy present at the boundaries of k-space in typical MR acquisitions. Then, by convolution theorem, $\boldsymbol{G}^H_{\text{conv}}$ is "diagonalizable" by a channel-wise Fourier transform, $\boldsymbol{G}^H_{\text{conv}} = \underline{\boldsymbol{F}}\boldsymbol{\Lambda}\underline{\boldsymbol{F}}^H$, where $\boldsymbol{\Lambda}$ is an operator that operates independently on pixels in the multi-channel image domain, not mixing information between pixel locations, i.e. $(\boldsymbol{\Lambda}\boldsymbol{x})[i] = \boldsymbol{\Lambda}_i(\boldsymbol{x}[i])$, for some $\boldsymbol{x} \in \mathbb{C}^{NC}$, with $\boldsymbol{\Lambda}_i \in \mathbb{C}^{C\times C}$, for $1 \le i \le N$. We can now describe the noise-covariance matrix of the coil-combined reconstructed image as,

$$\text{Cov}(\boldsymbol{y}) = \boldsymbol{S}^H\underline{\boldsymbol{F}}^H\boldsymbol{G}^H_{\text{conv}}(\boldsymbol{M}_{\Omega} \otimes \boldsymbol{\Sigma})\boldsymbol{G}_{\text{conv}}\underline{\boldsymbol{F}}\boldsymbol{S} \tag{S23}$$

$$= \boldsymbol{S}^H\boldsymbol{\Lambda}^H(\boldsymbol{F}^H\boldsymbol{M}_{\Omega}\boldsymbol{F} \otimes \boldsymbol{\Sigma})\boldsymbol{\Lambda}\boldsymbol{S} \tag{S24}$$

$$= \boldsymbol{S}^H\boldsymbol{\Lambda}^H(\boldsymbol{M}^{\text{conv}}_{\Omega} \otimes \boldsymbol{\Sigma})\boldsymbol{\Lambda}\boldsymbol{S}, \tag{S25}$$

where $\boldsymbol{M}_{\Omega}^{\text{conv}} = \boldsymbol{F}^H \boldsymbol{M}_{\Omega} \boldsymbol{F}$ is the channel-wise image-domain convolution operator defined by the k-space subsampling mask. This simplified formula for the covariance matrix makes it clear that the structure is **not diagonal**. The image-domain convolution operator will have A evenly spaced delta's corresponding to the uniform acceleration rate, with each delta scaled by $1/A$. The diagonal of the covariance matrix will thus be given by,

$$\boldsymbol{\sigma} = \sqrt{\frac{1}{A} \boldsymbol{S}^H \boldsymbol{\Lambda}^H \overline{\boldsymbol{\Sigma}} \boldsymbol{\Lambda} \boldsymbol{s}}. \tag{S26}$$

This expression can be obtained by considering passing the i-th column of the identity matrix through the full covariance operator, and only keeping the i-th entry.

GRAPPA is most commonly used in conjunction with auto-calibration signal (ACS) at the center of k-space. This ACS region is used as reference data to determine the weights of the GRAPPA interpolation kernel, and it is sensible to include this acquired signal as part of the final reconstruction. Recall the decomposition of the index set Ω into an $A\times$ uniform subsampling mask Ξ and an ACS region index set Θ which are not disjoint, i.e. $\Omega = \Xi \cup \Theta$ and $\Xi \cap \Theta \neq \emptyset$. We write the interpolation operator as, $\boldsymbol{G}^H = (\boldsymbol{G}_{\text{conv}}^H \underline{\boldsymbol{M}}_{\bar{\Theta}} + \underline{\boldsymbol{M}}_{\Theta}) \underline{\boldsymbol{I}}_{\Omega}^T$, where $\bar{\Theta}$ denotes the complement of set Θ. The resulting noise covariance matrix from this GRAPPA+ACS reconstruction can be described as,

$$\text{Cov}(\boldsymbol{G}^H \underline{\boldsymbol{I}}_{\Omega}^T \boldsymbol{k}) \tag{S27}$$

$$= \boldsymbol{G}^H (\boldsymbol{M}_{\Omega} \otimes \boldsymbol{\Sigma}) \boldsymbol{G} \tag{S28}$$

$$= (\boldsymbol{G}_{\text{conv}}^H \underline{\boldsymbol{M}}_{\bar{\Theta}} + \underline{\boldsymbol{M}}_{\Theta})(\boldsymbol{M}_{\Omega} \otimes \boldsymbol{\Sigma})(\underline{\boldsymbol{M}}_{\bar{\Theta}} \boldsymbol{G}_{\text{conv}} + \underline{\boldsymbol{M}}_{\Theta}) \tag{S29}$$

$$= \boldsymbol{G}_{\text{conv}}^H (\boldsymbol{M}_{\Omega \cap \bar{\Theta}} \otimes \boldsymbol{\Sigma}) \boldsymbol{G}_{\text{conv}} + (\boldsymbol{M}_{\Theta} \otimes \boldsymbol{\Sigma}). \tag{S30}$$

Hence the image-domain coil-combined noise covariance will be described by,

$$\text{Cov}(\boldsymbol{y}) = \boldsymbol{S}^H (\boldsymbol{\Lambda}^H (\boldsymbol{M}_{\Omega \cap \bar{\Theta}}^{\text{conv}} \otimes \boldsymbol{\Sigma}) \boldsymbol{\Lambda} + (\boldsymbol{M}_{\bar{\Theta}}^{\text{conv}} \otimes \boldsymbol{\Sigma})) \boldsymbol{S}. \tag{S31}$$

Clearly this matrix is not diagonal due to the presence of the image domain convolution operators $\boldsymbol{M}_{\Omega \cap \bar{\Theta}}^{\text{conv}}$ and $\boldsymbol{M}_{\bar{\Theta}}^{\text{conv}}$. However, we may reason about the diagonal of this covariance matrix by considering applying it to the i-th column of the identity. The convolution operators are our primary interest, as the operators $\boldsymbol{S}$, $\boldsymbol{\Lambda}$, and $\boldsymbol{\Sigma}$ are all pixel-wise (though perhaps spatially varying) operators, and thus do not contribute to introducing correlations. First, $\boldsymbol{M}_{\bar{\Theta}}^{\text{conv}}$ is the convolution operator corresponding to a low-pass filter in the phase-encoding direction with factional-width $p = |\Theta|/N$. Hence, $\boldsymbol{M}_{\bar{\Theta}}^{\text{conv}}$ is a sinc filter with peak amplitude p. Second, $\boldsymbol{M}_{\Omega \cap \bar{\Theta}}^{\text{conv}}$ can be rewritten as the filter operator corresponding to the k-space mask $\boldsymbol{M}_{\Omega \cap \bar{\Theta}} = \boldsymbol{M}_{\Xi}(\boldsymbol{I} - \boldsymbol{M}_{\Theta})$, i.e. the $A\times$ aliasing filter convolved with the impulse filter minus the p-amplitude sinc filter. This combined filter will have an amplitude of $(1-p)/A$ at its center. All together, thinking only about the i-th element of the result multiplication of the entire covariance matrix with the i-th column of the identity, we can arrive at the following image-domain coil-combined noise-level formula for an $A\times$ GRAPPA+ACS reconstruction,

$$\boldsymbol{\sigma} = \sqrt{\tfrac{1-p}{A} \cdot \boldsymbol{S}^H \boldsymbol{\Lambda}^H \overline{\boldsymbol{\Sigma}} \boldsymbol{\Lambda} \boldsymbol{s} + p \cdot \boldsymbol{S}^H \overline{\boldsymbol{\Sigma}} \boldsymbol{s}}. \tag{S32}$$

Again, we emphasize that this noise-level is simply the square-root of the diagonal of a non-diagonal noise-covariance matrix.

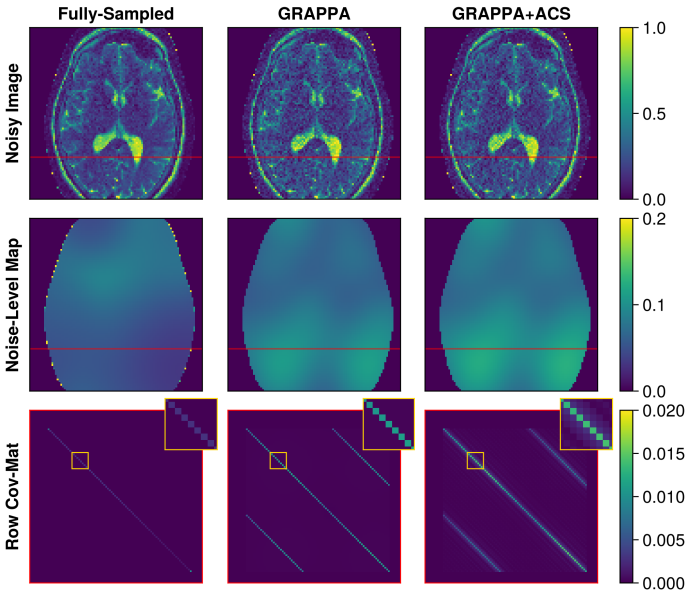

FIGURE S1 Noise covariance under fully-sampled, GRAPPA reconstructed, and GRAPPA+ACS reconstructed settings. **Row 1**: noisy images. **Row 2**: associated noise-level maps (square-root of noise covariance diagonal). **Row 3**: sub-matrix of noise-covariance matrix corresponding to a single row (highlighted in red) of the image. Zoomed in region on the covariance matrix highlights the existence of *local noise-correlations* in the GRAPPA+ACS reconstructed data, whereas fully-sampled and GRAPPA reconstructed data have zero off-diagonal elements or only nonlocal correlations, respectively. Image colorbars for are given on the right side for each row.

Supporting Information Figure S1 shows an example set of noisy images from fully-sampled, GRAPPA reconstructed, and GRAPPA+ACS reconstructed data, along with their associated noise-level maps (row 2), and a subset of the noise-covariance matrix between pixels of a single image row. To compute the covariance matrix, we passed columns of the identity matrix through the full covariance matrix expressions, given in Equations

(S25) and (S31). For computational reasons, we scaled our ground-truth data and synthetic-noise generation to an image-size of 96×96. Note that for Cartesian subsampling based GRAPPA reconstruction, noise correlations are introduced by subsampling in the phase-encoding direction of k-space, therefore noise-correlations only exist in image-space in that direction (in this case, only between pixels of a given row).

First, we note that the noise-covariance in the fully sampled case is diagonal *and* spatially varying. Next, we see that without the ACS signal the spatial correlation between pixels is long-range (the two off-diagonal bands in covariance matrix correspond to the $2\times$ aliasing pattern). However, inclusion of the ACS region smears these correlations with a 1D sinc-filter, introducing local spatial correlations in the image. This smearing effect can prove catastrophic in the case of SURE-based neural network training as the correlations are within the receptive field of each other, and thus violate the independence assumption of SURE.

5 | ADDITIONAL SYNTHETIC NOISE RESULTS

In this section, Supporting Information Figures S2 and S3 provide additional synthetic denoising results (corresponding to Experiments 1 and 2 in the main text).

ORCID
Nikola Janjušević 0000-0002-8277-3175
Jingjia Chen 0000-0002-6023-1033
Yao Wang 0000-0003-3199-3802
Li Feng 0000-0002-8692-7645

REFERENCES

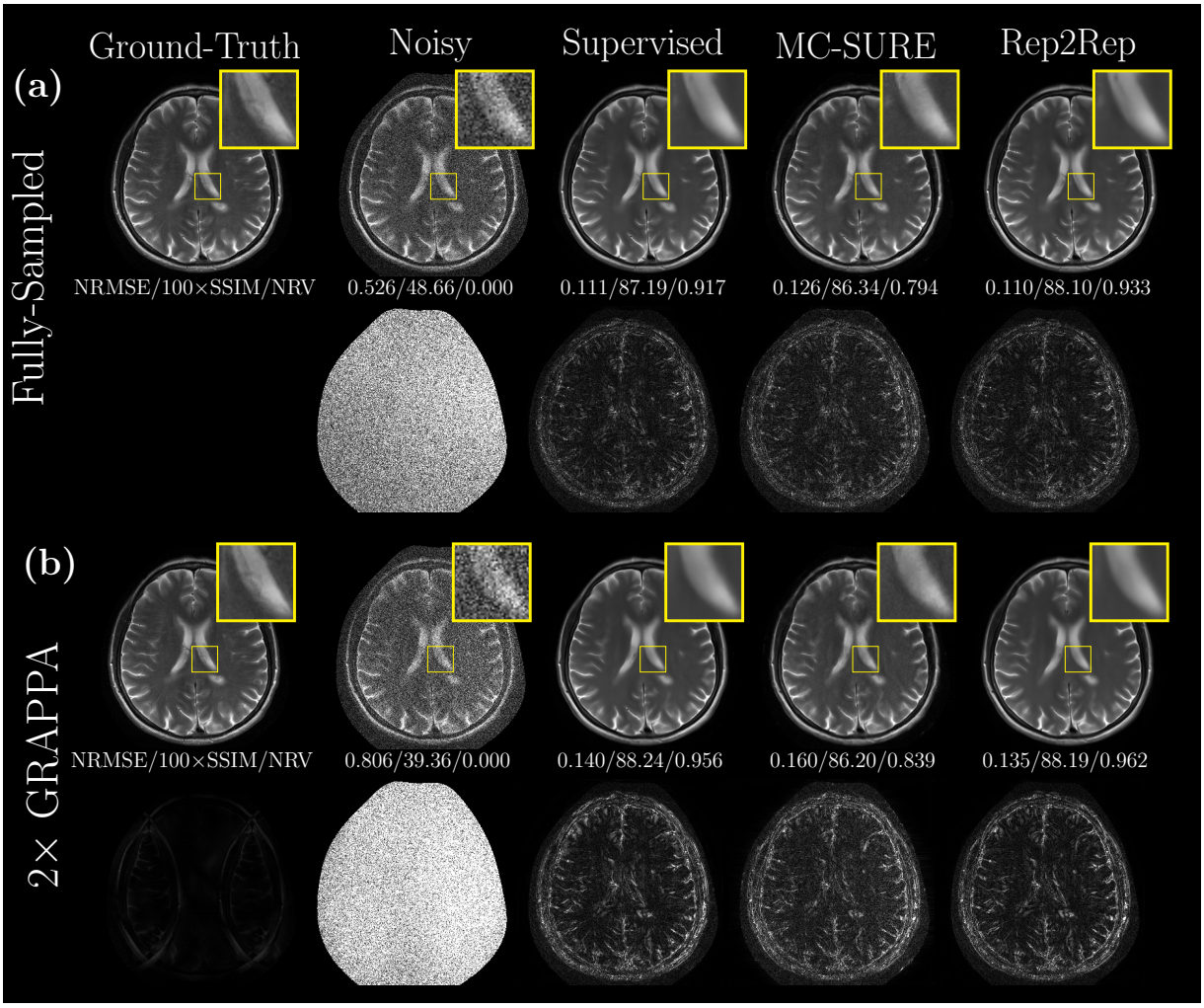

FIGURE S2 Visual comparison of CDLNet denoising under different training schemes on the synthetic-noise T2w fastMRI Brain dataset. (a) Denoising of fully-sampled noisy data. (b) Denoising of 2× GRAPPA reconstructed data (ACS included). 5× absolute denoising error is shown below each image. Quantitative metrics (NRMSE/100×SSIM/NRV) are shown below each image.

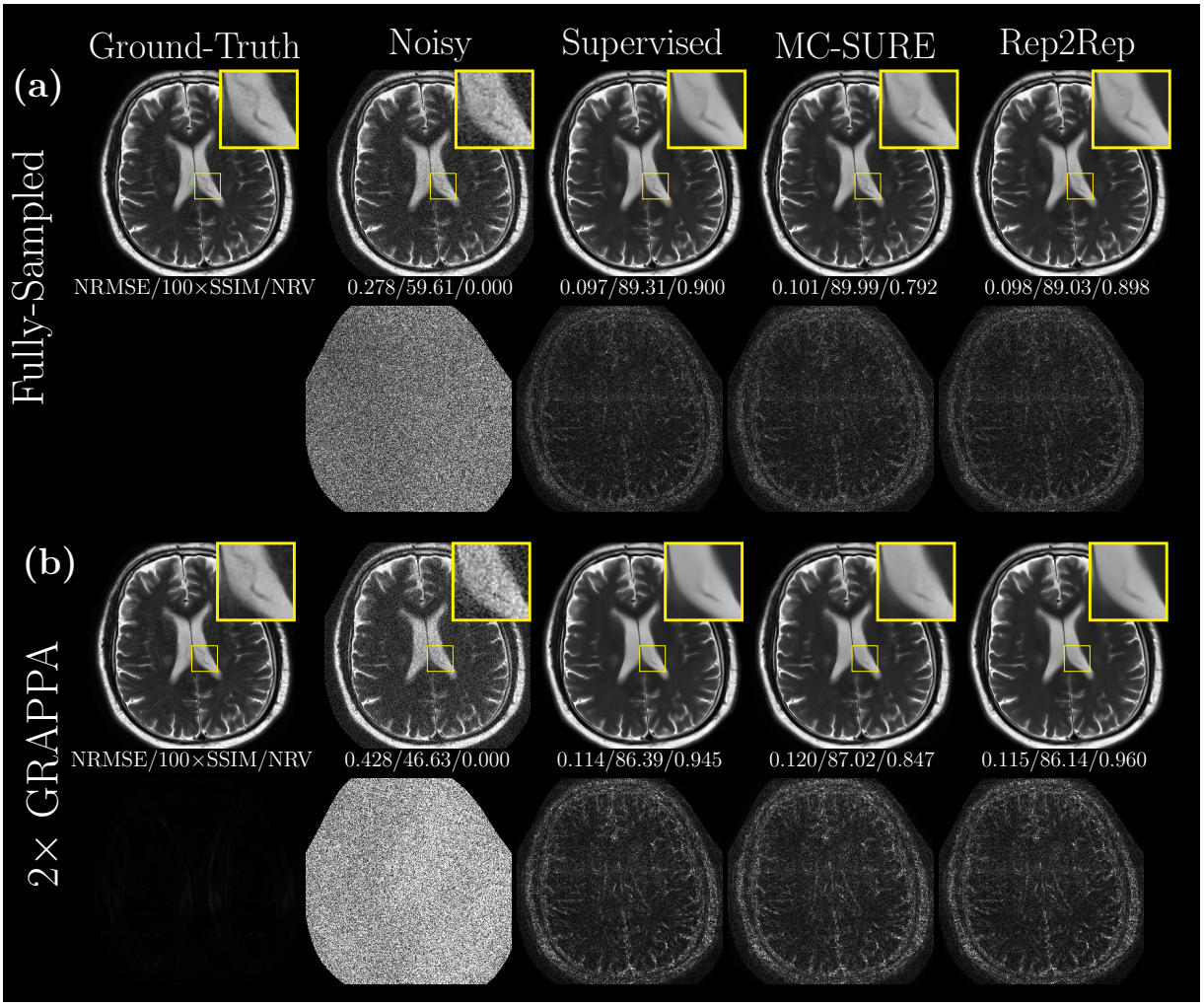

FIGURE S3 Visual comparison of CDLNet denoising under different training schemes on the synthetic-noise T2w fastMRI Brain dataset. (a) Denoising of fully-sampled noisy data. (b) Denoising of 2× GRAPPA reconstructed data (ACS included). 5× absolute denoising error is shown below each image. Quantitative metrics (NRMSE/100×SSIM/NRV) are shown below each image.